

Enhanced Stability and Fluidity in Droplet on Hydrogel Bilayers for Measuring Membrane Protein Diffusion

James R. Thompson,[†] Andrew J. Heron,[†] Yusdi Santoso,[‡] and Mark I. Wallace^{*†}

Physical and Theoretical Chemistry Laboratory, University of Oxford, Chemistry Research Laboratory, 12 Mansfield Road, Oxford, OX1 3TA, U.K., and Department of Physics, University of Oxford, Clarendon Laboratory, Parks Road, Oxford, OX1 3PU, U.K.

Received August 6, 2007; Revised Manuscript Received September 13, 2007

ABSTRACT

We form artificial lipid bilayers suitable for single-molecule fluorescence microscopy by contacting an aqueous droplet with a hydrogel support immersed in a solution of lipid in oil. Our results show that droplet on hydrogel bilayers (DHBs) have high lipid mobilities, similar to those observed in unsupported lipid bilayers. DHBs are also stable over a period of several weeks. We examine membrane protein diffusion in these bilayers and report a decreased lateral mobility of the heptameric β -barrel pore-forming toxin α -hemolysin versus that of its monomeric precursor. These results corroborate previous models of the α -hemolysin insertion mechanism where the monomer binds to the lipid bilayer without insertion.

Single-particle tracking (SPT) is a powerful technique for measuring dynamics and heterogeneity in biological systems.¹ In particular, the ability to observe single fluorescently-labeled molecules diffusing in and upon lipid bilayers has greatly improved our understanding of membrane biology.^{2–4} Although the majority of SPT experiments have been performed *in vivo*, it is also possible to study biomolecules in artificial bilayers, where the complicating effects of the natural membrane environment are removed. To date, experiments on artificial bilayers have yielded information about lipid dynamics on different supporting substrates^{5–7} and the rates of lateral diffusion of proteins.^{8–10} Artificial lipid bilayers can be either supported or unsupported and are formed using a number of different techniques. For fluorescence experiments, artificial bilayers are usually formed directly on a glass support (either by vesicle deposition or the Langmuir–Blodgett technique^{5,11}) or on intermediate substrates such as gels or polymers.^{9,12,13} Experiments studying artificial bilayer fluidity have shown that lateral mobilities of lipids in substrate-supported lipid bilayers (SLBs) are in general considerably lower than those observed for unsupported bilayers.⁷ The interaction between the solid support and bilayer may hinder the lateral mobility of lipids and hence could potentially affect protein function. Substrate-supported bilayers are also often limited by inhomogeneity

of the bilayer.¹⁴ Despite these drawbacks, supported lipid bilayers offer the principle advantage of being straightforward to image.

Unsupported artificial bilayers have been used for single-molecule fluorescence experiments; however, it is not easy accommodating single-molecule fluorescence imaging, using either total internal reflection fluorescence (TIRF) microscopy^{10,15} or epifluorescence microscopy.^{10,16} Techniques used to create such bilayers are sometimes difficult to work with and experiments are often limited by short bilayer lifetimes. New methods for generating artificial membranes have recently been reported where a lipid bilayer is formed by contacting two aqueous phases immersed under a solution of lipid in oil.^{17–19} We have shown that artificial bilayers formed between an aqueous droplet and a hydrogel immersed in a solution of lipid in oil are amenable to electrical recording of membrane channels.²⁰ These droplet on hydrogel bilayers (DHBs) show high (>100 G Ω) electrical seals, suitable for single-channel recording.

Here, we show DHBs can be used for single-molecule fluorescence microscopy and apply the technique to characterize the lipid bilayer and to probe the insertion mechanism of the β -barrel pore-forming toxin α -hemolysin. DHBs also exhibit enhanced stability compared to other artificial bilayer methods, with bilayers being stable over several weeks. DHBs are created on thin hydrogel supports by depositing a layer of molten agarose, which after drying can be rehydrated, leaving an ultrathin planar gel support. A thin

* Corresponding author. Email: mark.wallace@chem.ox.ac.uk.

[†] Physical and Theoretical Chemistry Laboratory, University of Oxford.

[‡] Department of Physics, University of Oxford.

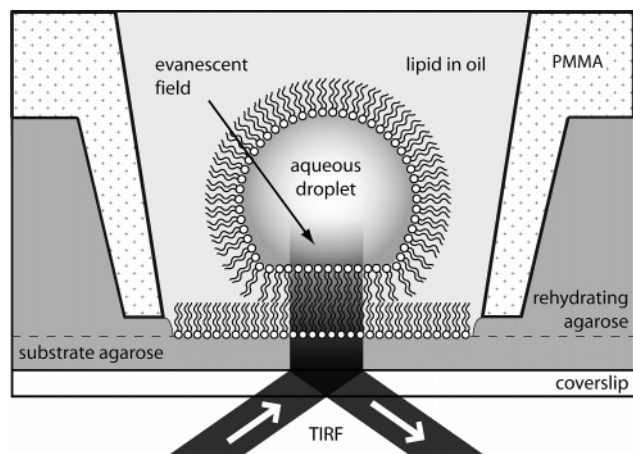


Figure 1. A schematic diagram of TIRF microscopy on DHBs. A supporting substrate comprised of a thin layer of agarose (≈ 200 nm in thickness) is formed on a glass coverslip. This thin substrate film is rehydrated by filling a poly(methyl methacrylate) micro-channel device with aqueous agarose. The device wells are filled with a solution of lipid in oil. An aqueous droplet (approximately 50 nL in volume) is placed on top of the hydrogel underneath the oil. A lipid bilayer (approximately $200 \mu\text{m}$ in diameter) forms at the interface between the two aqueous phases. The evanescent field propagates into the DHB illuminating the lipid bilayer and fluorophore-tagged biomolecules in the droplet.

supporting gel layer is critical for TIRF illumination through to the lipid bilayer. A diagram of our experimental approach is shown in Figure 1. Using TIRF microscopy and single-particle tracking, we measure the lateral diffusion of fluorescently-labeled lipids and observe essentially identical DHB lipid mobility as is observed in unsupported bilayers. We examine the diffusion of the β -barrel pore-forming toxin, α -hemolysin, at two different stages of its assembly pathway. α -Hemolysin is secreted by the human commensal *Staphylococcus aureus* as a water soluble monomer.²¹ Upon binding to target membranes it assembles to form a transmembrane β -barrel pore.²² This spontaneous assembly makes α -hemolysin a useful system with which to study protein oligomerization and β -barrel insertion.²³

Droplet on Hydrogel Bilayer Characterization. We have characterized DHBs by calculating the lateral diffusion coefficients of lipids from averaged mean-square displacement (MSD) versus Δt plots. The average MSD versus Δt for all tracks are shown in Figure 2 and these data were fitted with a linear function weighted by the standard deviation calculated for each time lag. Data were fitted over all track lengths (maximum 287.5 ms). Figure 2 shows the first 30 ms to highlight the difference between species. DHB lipids show considerably greater mobility than supported lipid bilayers with an approximately 20-fold higher lateral diffusion coefficient. The D_{lat} value for DHBs ($D_{\text{lat}} = 26.8 \pm 7.1 \mu\text{m}^2 \text{s}^{-1}$) is comparable to previous unsupported 1-palmitoyl 2-oleoyl phosphatidylcholine lipid bilayer SPT measurements ($D_{\text{lat}} = 20.6 \pm 0.9 \mu\text{m}^2 \text{s}^{-1}$).⁷ The difference between our SLB and DHB values is very similar to the ratio of D_{lat} values derived from comparison of other supported⁵ and unsupported⁷ lipid bilayer SPT measurements.

Individual MSD versus Δt_n were also calculated for all tracks with their resultant D_{lat} values shown as histograms

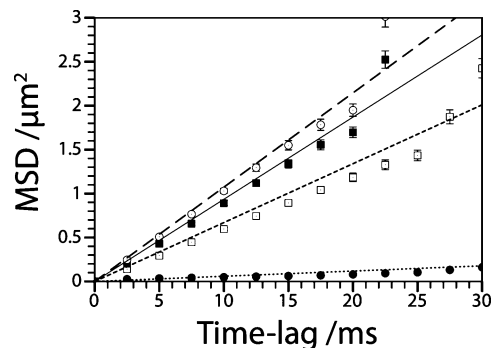


Figure 2. Mean MSD versus time lag for all experimental data for each diffusing species studied. SLB lipid (solid circles) with corresponding weighted linear fit (dotted line) shows the slowest lateral diffusion coefficient ($D_{\text{lat}} = 1.5 \pm 0.5 \mu\text{m}^2 \text{s}^{-1}$). DHB lipid (open circles) with corresponding weighted linear fit (large-dashed line) shows the fastest lateral diffusion coefficient ($D_{\text{lat}} = 26.8 \pm 7.1 \mu\text{m}^2 \text{s}^{-1}$). αHL_1 (solid squares) with corresponding weighted linear fit (solid line) shows the fastest lateral diffusion coefficient of the two proteins ($D_{\text{lat}} = 23.4 \pm 6.4 \mu\text{m}^2 \text{s}^{-1}$). Finally, αHL_7 (open squares) with corresponding weighted linear fit (small-dashed line) shows the slowest lateral diffusion coefficient of the two proteins ($D_{\text{lat}} = 16.8 \pm 4.2 \mu\text{m}^2 \text{s}^{-1}$). Error bars show the standard error of the mean for the averaged data.

Table 1. Fitting Results for Probability Distributions in Supporting Information, Figure 3

	diffusing species	number of trajectories	α_1	$r_1^2 / \mu\text{m}^2$	$r_2^2 / \mu\text{m}^2$
A	SLB lipid	1050	0.94 ± 0.02	0.11 ± 0.02	1.78 ± 0.65
B	DHB lipid	844	0.08 ± 0.04	0.65 ± 1.11	7.25 ± 0.19
C	αHL_1	894	0.17 ± 0.07	1.64 ± 1.05	7.15 ± 0.30
D	αHL_7	909	0.78 ± 0.16	3.21 ± 0.46	8.44 ± 2.53

in Figure 3. These data were found to fit to a gamma distribution, as expected for two-dimensional Brownian diffusion.^{24,25} The mean values of which mirror the trend observed in the MSD versus Δt_n calculations.

D_{lat} values are affected by the length scale and the temporal resolution of the experiment.^{7,26} Techniques used to measure diffusion at smaller length scales than SPT yield considerably faster D_{lat} values,²⁶ whereas experiments with longer length scales yield slower D_{lat} values.^{7,26} We see a similar trend whereupon a reduction in our lateral resolution we observe that the calculated D_{lat} values increase (data not shown). We report a higher D_{lat} value for DHB lipids from an experiment with a smaller length scale and with an increased time resolution than prior SPT experiments on lipid diffusion.⁷

We also analyzed the track populations for multiple mobility components. The probability of diffusion was calculated according to Schmidt and co-workers^{6,7} with the fitting parameters given in Table 1. We see two mobility components in all species observed. Ninety-four percent of SLB lipid displacements belonged to the slower mobility component (α_1) in contrast with lipids in DHBs where only an 8% fraction belong to this slow component. This analysis suggests that DHBs contain only a very small fraction of slowly diffusing lipids in contrast to the much larger proportion of slower diffusing lipids in SLBs. This is likely due to a reduction in surface interaction effects in the

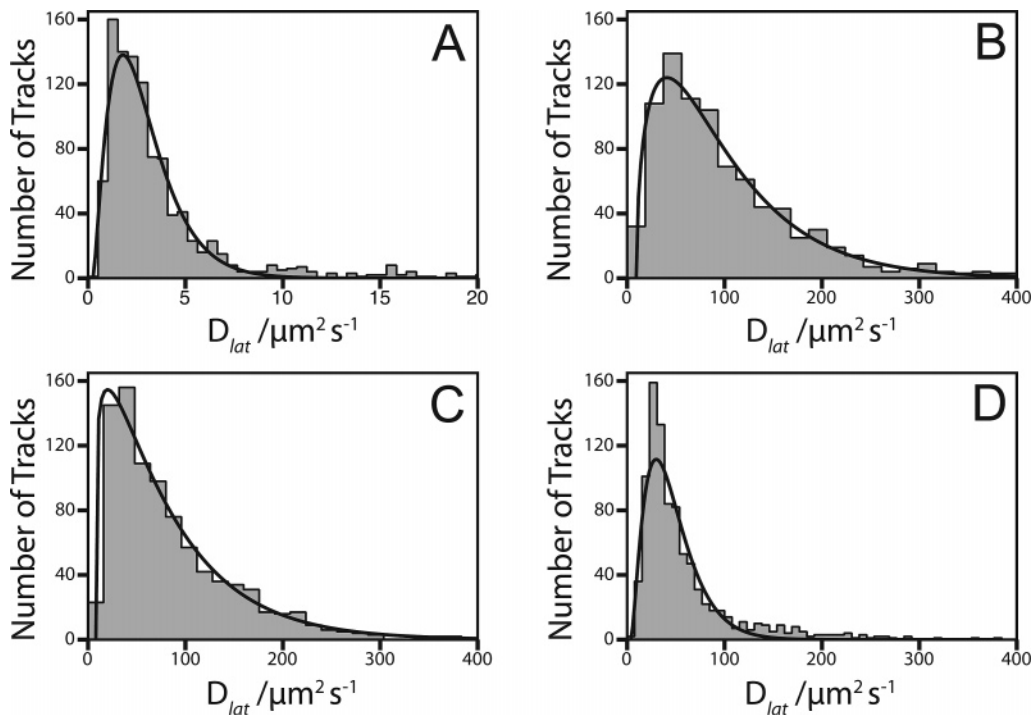


Figure 3. Histograms of individual track lateral diffusion coefficients with fitted probability density functions of the gamma distribution. (A) SLB lipid $\langle D_{lat} \rangle = 2.6 \mu\text{m}^2 \text{s}^{-1}$, $\chi_r^2 = 2.1$. (B) DHB lipid $\langle D_{lat} \rangle = 90.0 \mu\text{m}^2 \text{s}^{-1}$, $\chi_r^2 = 1.1$. (C) αHL_1 $\langle D_{lat} \rangle = 75.0 \mu\text{m}^2 \text{s}^{-1}$, $\chi_r^2 = 0.8$. (D) αHL_7 $\langle D_{lat} \rangle = 42.7 \mu\text{m}^2 \text{s}^{-1}$, $\chi_r^2 = 2.3$.

presence of a supporting hydrogel.⁷ Although not entirely monoexponential, which would indicate absolute homogeneity,^{6,7} this slow-moving fraction in DHBs is clearly far smaller than in conventional SLBs.

We also attempt to quantify the stability of DHBs. In a simple experiment with 20 DHBs, each forming within 1 min of contacting a planar 1% agarose gel made with ultrapure water, all were still intact 2 weeks later. The only obvious difference was a shrinking of volume by approximately 25%. This is likely due to droplet dehydration where water partitions into the surrounding oil. Montal–Mueller bilayers are often fragile and difficult to create,²⁷ whereas in our experiments we are able to rapidly form bilayers that are extremely stable, enabling experiments over much longer time courses.

α -Hemolysin Analysis. Both the MSD versus Δt_n analysis and histogram of D_{lat} values show that the lateral diffusion of fully inserted mature αHL_7 is lower than that shown for αHL_1 . Eighty-three percent of the αHL_1 displacements belong to the fast mobility component (α_2) with a D_{lat} value almost identical to the DHB lipid D_{lat} . This supports the hypothesis that αHL_1 only interacts with the upper leaflet of the bilayer.²⁸ αHL_7 shows a much larger proportion (78%) of displacements belonging to the slower component (α_1). We do not observe a similar slow component in αHL_7 , as seen in αHL_1 ; instead, the two components have much higher mobilities. We attribute the fastest component to free dye or noninserted heptamers diffusing in solution above the bilayer, as a result of the purification procedure required for αHL_7 . We attribute the slower component (α_1) in αHL_7 to the inserted heptamer and can hence compare its behavior with that seen for the fast component (α_2) in αHL_1 .

Experiments in model systems show that diffusional rates of a protein weakly depend on the reciprocal of the radius of the embedded portion of the protein.²⁹ As a result, we expect the major cause of the slowing of diffusion to be the insertion of the β -barrel across the membrane. In the case of α -hemolysin, the β -barrel is approximately 5 nm in diameter,²² which interacts with the lipid bilayer to a much greater extent than the monomeric precursor, for which it has been postulated that it only transiently adsorbs to the surface.²⁸ This model is consistent with the dramatic change in α -hemolysin diffusion that we observe. Following the approach of Sackmann and co-workers³⁰ with the assumptions laid out by Tamm,³¹ it is possible to assess the degree of penetration through the lipid bilayer membrane from D_{lat} values. With the gross approximation that the D_{lat} value for DHB lipids corresponds to zero insertion and the D_{lat} value for αHL_7 corresponds to complete insertion, we estimate that αHL_1 penetrates less than 5% of the depth of the bilayer. Without further supporting evidence, it is not possible to more accurately gauge the degree of bilayer penetration, as the radius of the membrane-interacting portion of the monomer is unknown. Our results suggest that a water-facing surface of αHL_1 interacts by binding to the lipid bilayer surface without significant protrusion of any protein domains into the bilayer.

We show that it is possible to make single-molecule fluorescence measurements on lipids and proteins diffusing in DHBs using TIRF microscopy. We characterize the fluidity of SLBs and DHBs using a tracking procedure based around the astronomical algorithm CLEAN (see Supporting Information). Lateral diffusion calculations indicate that DHB lipid mobilities are similar to those reported for unsupported

bilayers with negligible surface interactions, which are thought to typically hinder SLB lipid mobility. The enhanced stability and reproducibility of DHBs means that they are well suited to diffusion measurements on membrane bound or embedded molecules in vitro. Given that DHBs are amenable to single-channel electrical recording,²⁰ we envisage that this technique may provide a straightforward platform for reproducible simultaneous single-channel electrical recording and single-molecule fluorescence experiments. Previous experiments by different groups have begun to show that this simultaneous approach to biological measurements can yield insights into aspects of protein conformational dynamics while monitoring their activity.^{10,16,32–35} This would be of particular interest in the study of bacterial pore-forming toxin assembly such as that of α -hemolysin.

Acknowledgment. We thank H. Bayley for helpful discussions. Financial support for this project was provided by the BBSRC, EPSRC, and the Life Sciences Interface Doctoral Training Centre at the University of Oxford. Y.S is the holder of a Nanyang Technological University Overseas Scholarship. M.I.W. is a Royal Society University Research Fellow. Microscope apparatus was supported by Nikon Instruments U.K. as a part of the NOMIC partnership.

Supporting Information Available: Methods, tracking experiments, and data analysis. This material is available free of charge via the Internet at <http://pubs.acs.org>.

References

- (1) Saxton, M. J.; Jacobson, K. *Annu. Rev. Biophys. Biomol. Struct.* **1997**, *26*, 373–399.
- (2) Kusumi, A.; Sako, Y.; Yamamoto, M. *Biophys. J.* **1993**, *65*, 2021–2040.
- (3) Perez, J.-B.; Segura, J.-M.; Abankwa, D.; Piguet, J.; Martinez, K. L.; Vogel, H. *J. Mol. Biol.* **2006**, *363*, 918–930.
- (4) Lommerse, P. H. M.; Vastenhoud, K.; Pirinen, N. J.; Magee, A. I.; Spaink, H. P.; Schmidt, T. *Biophys. J.* **2006**, *91*, 1090–1097.
- (5) Schmidt, T.; Schütz, G. J.; Baumgartner, W.; Gruber, H. J.; Schindler, H. *Proc. Natl. Acad. Sci. U.S.A.* **1996**, *93*, 2926–2929.
- (6) Schütz, G. J.; Schindler, H.; Schmidt, T. *Biophys. J.* **1997**, *73*, 1073–1080.
- (7) Sonnleitner, A.; Schutz, G.; Schmidt, T. *Biophys. J.* **1999**, *77*, 2638–2642.
- (8) Ichikawa, T.; Aoki, T.; Takeuchi, Y.; Yanagida, T.; Ide, T. *Langmuir* **2006**, *22*, 6302–6307.
- (9) Wagner, M. L.; Tamm, L. K. *Biophys. J.* **2001**, *81*, 226–275.
- (10) Ide, T.; Takeuchi, Y.; Aoki, T.; Yanagida, T. *Jpn J. Physiol.* **2002**, *52*, 429–434.
- (11) Cremer, P. S.; Boxer, S. G. *J. Phys. Chem. B* **1999**, *103*, 2554–2559.
- (12) Goennenwein, S.; Tanaka, M.; Hu, B.; Moroder, L.; Sackmann, E. *Biophys. J.* **2003**, *85*, 646–655.
- (13) Tanaka, M.; Sackmann, E. *Nature* **2005**, *437*, 656–663.
- (14) Kühner, M.; Tampé, R.; Sackmann, E. *Biophys. J.* **1994**, *67*, 217–226.
- (15) Ide, T.; Yanagida, T. *Biochem. Biophys. Res. Commun.* **1999**, *265*, 595–599.
- (16) Borisenko, V.; Lougheed, T.; Hesse, J.; Füreder-Kitzmüller, E.; Fertig, N.; Behrends, J. C.; Woolley, G. A.; Schütz, G. *J. Biophys. J.* **2003**, *84*, 612–622.
- (17) Malmstadt, N.; Nash, M. A.; Purnell, R. F.; Schmidt, J. J. *Nano Lett.* **2006**, *6*, 1961–1965.
- (18) Funakoshi, K.; Suzuki, H.; Takeuchi, S. *Anal. Chem.* **2006**, *78*, 8169–8174.
- (19) Holden, M. A.; Needham, D.; Bayley, H. *J. Am. Chem. Soc.* **2007**, *129*, 8650–8655.
- (20) Heron, A. J.; Thompson, J. R.; Mason, A. E.; Wallace, M. I. *J. Am. Chem. Soc.* Accepted for publication.
- (21) Bhakdi, S.; Tranum-Jensen, J. *Microbiol. Rev.* **1991**, *55*, 733–751.
- (22) Song, L.; Hobough, M. R.; Shustak, C.; Cheley, S.; Bayley, H.; Gouaux, J. E. *Science* **1996**, *274*, 1859–1866.
- (23) Bayley, H.; Jayasinghe, L.; Wallace, M. *Nat. Struct. Mol. Biol.* **2005**, *12*, 385–386.
- (24) Saxton, M. J. *Biophys. J.* **1997**, *72*, 1744–1753.
- (25) Qian, H.; Sheetz, M. P.; Elson, E. L. *Biophys. J.* **1991**, *60*, 910–921.
- (26) Vaz, W. L.; Almeida, P. F. *Biophys. J.* **1991**, *60*, 1553–1554.
- (27) Montal, M.; Mueller, P. *Proc. Natl. Acad. Sci. U.S.A.* **1972**, *69*, 3561–3566.
- (28) Walker, B.; Krishnasastri, M.; Zorn, L.; Bayley, H. *J. Biol. Chem.* **1992**, *267*, 21782–21786.
- (29) Gambin, Y.; Lopez-Esparza, R.; Reffay, M.; Sierecki, E.; Gov, N. S.; Genest, M.; Hodges, R. S.; Urbach, W. *Proc. Natl. Acad. Sci. U.S.A.* **2006**, *103*, 2098–2102.
- (30) Evans, E.; Sackmann, E. *J. Fluid Mech.* **1988**, *194*, 553–561.
- (31) Tamm, L. K. *Biochim. Biophys. Acta* **1991**, *1071*, 123–148.
- (32) Harms, G.; Orr, G.; Lu, P. *Appl. Phys. Lett.* **2004**, *84*, 1792–1794.
- (33) Chandler, E. L.; Smith, A. L.; Burden, L. M.; Kasianowicz, J. J.; Burden, D. L. *Langmuir* **2004**, *20*, 898–905.
- (34) Peng, S.; Publicover, N. G.; Kargacin, G. J.; Duan, D.; Airey, J. A.; Sutko, J. L. *Biophys. J.* **2004**, *86*, 134–144.
- (35) Demuro, A.; Parker, I. *Biophys. J.* **2004**, *86*, 3250–9.

NL071943Y